Arabian Journal of Geosciences (2021) 14: 1115
https://doi.org/10.1007/s12517-021-07502-8

ORIGINAL PAPER

Radiological hazards assessment due to natural radioactivity in soils from Imereti region (Georgia)

Kakhaber Kapanadze[1] · Archil Magalashvili[1] · Platon Imnadze[2]

Received: 18 December 2020 / Accepted: 1 June 2021 / Published online: 7 June 2021

Abstract

The aim of the research is to investigate the spread of radioactive sources in the soils of the Dzirula crystalline massif (Western Georgia), taking into account its geological characteristics, as well as to determine the main radiological parameters that assess the risks of exposure to the population living in the study area. Using the gamma spectroscopy method, activity concentrations of primordial radionuclides ^{40}K, ^{238}U, and ^{232}Th are measured in various samples. Activity concentrations of the technogenic radionuclide ^{137}Cs are determined along with natural radionuclides, which makes it possible to assess the quality of artificial radioactive contamination of the study area. The measured activity concentrations vary in the range of 636–1260 for ^{40}K, 33–54 for ^{238}U, 34–82 for ^{232}Th, and 12–46 Bq/kg for ^{137}Cs. The gamma absorbed dose rates in the air are in the range of 66–122 nGy/h, with a mean value of 97 nGy/h, while the outdoor annual effective dose rates are in the range of 0.08–0.015 mSv/y. The average value of radium equivalent activity is 203 Bq/kg. The calculated values of the external hazard index (H_{ex}) are in the range of 0.37–0.70. It has been shown with a significant degree of reliability that here soils with relatively increased natural radioactivity are products of the weathering of sialic (granite) rocks of the crystalline massif, while soils with low radioactivity are the product of sedimentary and mafic rocks. This data is well correlated with the results of a similar study of the other — Khrami crystalline massif of Georgia. Obtained results are compared with the studies conducted for some other regions of Georgia and the world, as well as with limitations and recommendations established by the relevant international organizations. Comparison of the results shows that the radioactive characteristics of the study area are slightly increased, but remain within the recommended limits.

Keywords Natural radioactivity · Soil · Dzirula massif · Radiological hazards

Introduction

Radionuclides naturally occurring in soils make an important contribution to human irradiation. According to UNSCEAR, most of the total radiation is caused by natural sources (UNSCEAR 2000). Therefore, to assess the risks of irradiation, a detailed study of natural sources of radiation in soils is important and evident. Main part of terrestrial gamma radiation is caused by natural radionuclides, such as ^{40}K, ^{238}U, ^{232}Th, and their progenies distributed in the soil.

The radioactivity of the soil depends on the content and distribution of natural radioisotopes in it, while the latter depends on soil parent material and some other factors of soil formation. As a rule, relatively high level of natural radioactivity is related with magmatic rocks (e.g., granite) and the low level with sedimentary rocks. Differences are also observed in the igneous rocks themselves, for example, felsic igneous rocks are characterized by a relatively higher content of natural radioisotopes than ultramafic and mafic igneous rocks (Dhawal et al. 2013).

In Georgia, rocks with granite composition are mainly represented in the axial part of the Great Caucasus Mountains and in the crystalline missives — Dzirula, Khrami, and Loki, which represent the salients of old (Variscan) terrain of the so-called Georgian massif (Adamia et al. 2011). Our previous

Responsible Editor: Amjad Kallel

✉ Kakhaber Kapanadze
kakhaberi.kapanadze.2@iliauni.edu.ge

[1] School of Natural Sciences and Medicine, Ilia State University, Tbilisi, Georgia

[2] Applied Research Centre Laboratory of Radiological Studies, Andronikashvili Institute of Physics of Javakhishvili Tbilisi State University, Tbilisi, Georgia

research is devoted to the Khrami crystalline massif (Kapanadze et al. 2019). Some studies are conducted for other regions of Georgia by other authors (Kekelidze et al. 2017; Kekelidze et al. 2018). In present research, the part of Dzirula massif is selected, which is the highest and most fragmented area of the Imereti (Upper Imereti) region of western Georgia and is characterized by humid subtropical climate and well-developed soil-forming processes. During the selection of the study area, in addition to petrology, other factors are taken into account as well, for instance, existence of settlements in the region, agriculture, and mining activities.

Materials and methods

Characteristics of the study area

The study area occupies about 100 km^2 and includes parts of the river Dzirula and its tributaries basin in the Upper Imereti region. Yellow brown forest soils of different granulometry are predominant in the study area (Urushadze et al. 2015).

Based on the existing geological data (Geguchadze et al. 1972), the rocks in the study area are mainly represented by granitoids (Middle Jurassic), quartz-diorites, microclinized granitoids and migmatites (Late-Middle Paleozoic), microcline (rose) granites (Middle Paleozoic), and gabbroic rocks (Paleozoic). Mesozoic-Cenozoic sedimentary rocks (marls, limestones, sandstones, etc.) adjacent to the Dzirula massif are also sporadically presented in the study area (Fig. 1).

Sampling methodology

To ensure comparability of research results, well-proven methodology, used also in previous research (Kapanadze et al. 2019), is used in the present study. Considering geological peculiarities of the study area, a specific sampling scheme has been developed. The samples were taken at a reasonable distance from buildings and other artificial structures to exclude any appearance of nonlocal amount of soil in the samples. To present the nature of the local terrestrial radioactivity uniformly, systematic grid method (Mehdi et al. 2016) of soil sampling has been used. According to the sampling methodology, five samples (45–50 m apart) were collected in each sampling site and averaged. A total of 19 mixed samples were taken, which amounted to 95 samples. Sampling sites themselves were, on average, 1000 m apart. Each sample was taken at a depth of 5–20 cm from the soil surface, as most of impact from terrestrial radiation comes from the top layers of the soil (Dhawal et al. 2013). Initial processing of samples has been performed on site and, consequently, up to 500 g of soil fraction was obtained and sealed.

Laboratory measurements

Gamma spectroscopy, as a well-known technique, is used to define the activity concentrations of radionuclides in the soil samples. For the gamma spectroscopy analysis, samples have been prepared in accordance with approved and tested methodologies. Primarily, samples have been air dried and sifted to get them almost in powder form (weighing up to 150 g). Then samples have been sealed hermetically and stored for about 2 months, to attain equilibrium of ^{214}Bi and ^{214}Pb with ^{222}Rn (Kapanadze et al. 2019). Taking into account the storage period, it can be assumed that ^{228}U and ^{226}Ra reach the equilibrium (Keser et al. 2013; Rahman et al. 2012).

Measurements of the activity concentrations of radionuclides in soil samples have been conducted at the Institute of Physics of Tbilisi State University. CANBERRA high-purity germanium detector (HPGe) coupled with multichannel analyzer (MCA) has been used for laboratory works. ISOCS and LaBOCS software have been used for detector calibration. The detector has been calibrated using standard sources with known energies such as ^{137}Cs (662 keV), ^{60}Co (1173 keV and 1332 keV), and ^{241}Am (59 keV). The full width half maximum (FWHM) resolution of the detector at 1332 keV of ^{60}Co gamma ray was 1.8 keV. To reduce background effects, the detector is covered with a lead shield (10-cm thick). Genie-2000 software has been used for gamma spectrum analysis. Correction in each measurement has been made by subtraction of background levels. The counting time (to collect the spectrum for each sample) was 25000 s. To determine activity concentrations of ^{137}Cs and ^{40}K, single peaks of 662 keV and 1461 keV have been used respectively. Activity concentration of ^{238}U has been determined by measuring the 609 keV peak from ^{214}Bi and 352 keV peak from ^{214}Pb. Activity concentration of ^{232}Th has been determined by measuring 583 keV peak from ^{208}Tl and 911 keV peak from ^{228}Ac (Kapanadze et al. 2019).

Results of activity concentrations are calculated by using Eq. (1) (Kapanadze et al. 2019):

$$A_{Ei} = \frac{C_{Ei}}{D_{eff} \cdot \gamma \cdot t \cdot m} \quad (1)$$

where A_{Ei} is the activity concentration of the radionuclide i for a peak at energy E, C_{Ei} is the total count of a photopeak, D_{eff} is efficiency of detection, γ is the percentage of gamma emission probability, t is the counting time, and m is the mass of the sample (Kapanadze et al. 2019).

To determine contents of radionuclides (in ppm), following Eq. (2) is used (Knoll 1989):

$$m\ (ppm) = (A\ M / N_{Av}\ \ln 2)\ t_{1/2} \quad (2)$$

where A is activity concentration in (Bq/g) of the matter or daughter in radioactive equilibrium, M is molecular weight

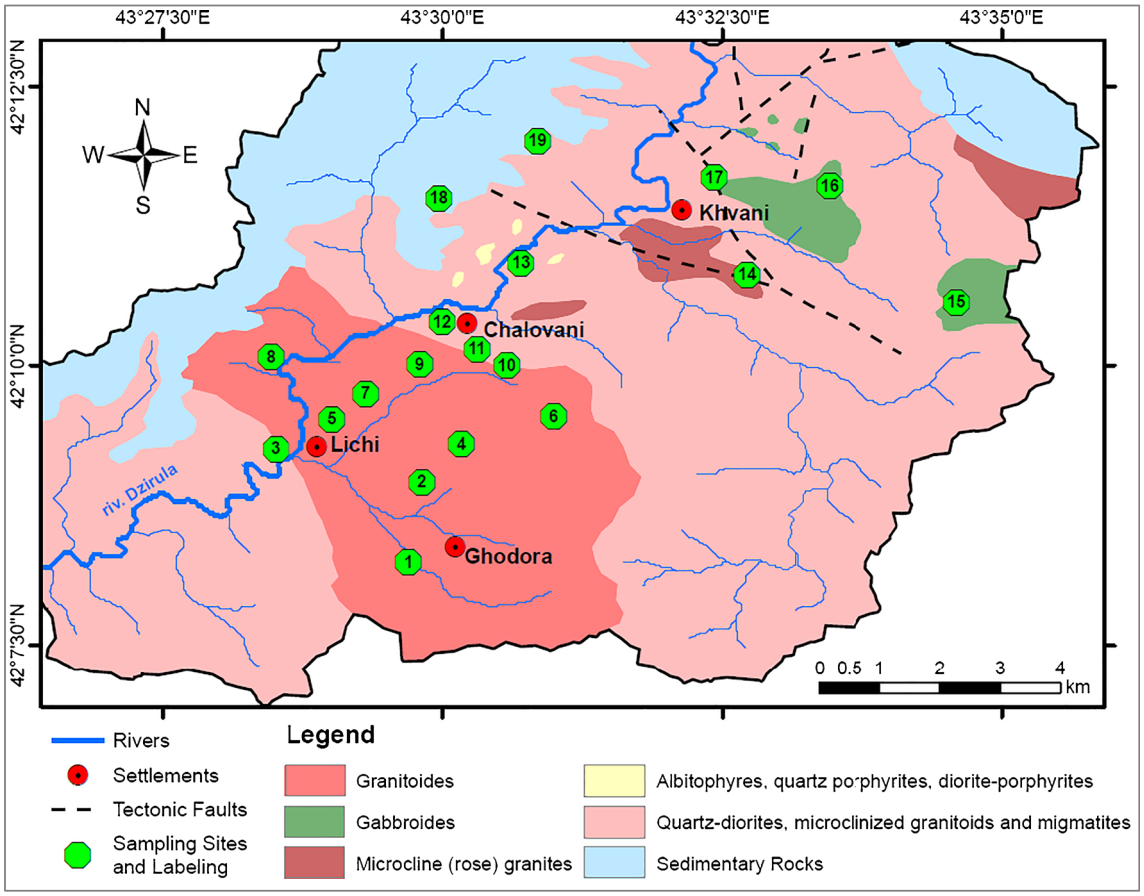

Fig. 1 Geological map of the study area (based on (Geguchadze et al. 1972))

(g/mol), N_{Av} is Avogadro's number (6.02×10^{23}), and $t_{1/2}$ is half-life in seconds.

Results and discussion

Radionuclide concentrations

The results of activity concentrations (in Bq/kg) and calculated contents (in ppm) of natural radionuclides ^{40}K, ^{238}U, and ^{232}Th as well as technogenic radionuclide ^{137}Cs are provided in Table 1. Apart from radionuclide concentrations, Table 1 also presents local characteristics of the sampling sites such as petrology, soil type, and altitude.

According to the results presented in Table 1, the average values of activity concentrations are 994, 44, and 58 Bq/kg for ^{40}K, ^{238}U, and ^{232}Th respectively. World median values of ^{40}K, ^{238}U, and ^{232}Th activity concentrations are 400, 35, and 30 Bq/kg respectively (UNSCEAR 2000). Comparison of obtained results with world median values shows that for ^{40}K, our results exceed world median value by 594 Bq/kg, for ^{238}U — by 9 Bq/kg, and for ^{232}Th — by 28 Bq/kg.

Activity concentrations of ^{137}Cs vary in range from 12 to 46 Bq/kg, with the average value of 27 Bq/kg. The maximum value of activity concentrations of ^{137}Cs (46 Bq/kg) is recorded at the 11th site (as well as for ^{238}U and ^{232}Th). Table 2 compares obtained results for ^{137}Cs with some studies conducted in Georgia and in various countries. According to the investigations carried out in Georgia, it is considered that average background values of the ^{137}Cs concentrations in the soils vary in the range from 1 to 10 Bq/kg for the whole territory of Georgia (Kekelidze et al. 2017). We assume that the sufficiently appreciable quantities for ^{137}Cs, in our results, indicate the trace, left after Chernobyl 1986 accident, and atmospheric weapon tests in the 1950s and 1960s. However, it is clear that some places of the study area and especially highland regions were relatively more polluted by technogenic radionuclides than eastern and lowland regions of the country. Generally, fallout and sedimentation of technogenic radionuclides after the Chernobyl accident depended on peculiarities of atmospheric circulations. Apparently, due to the kind of high-altitude barrier for the atmospheric currents and relatively high intensity of precipitation, contamination in the highlands is higher than in the lowlands.

Table 1 Radionuclide concentrations and characteristics of sampling sites

Site #	Activity concentrations (Bq/kg)				Contents (ppm)				Petrology	Soil type	Altitude (m)
	^{40}K	^{238}U	^{232}Th	^{137}Cs	^{40}K	^{238}U	^{232}Th	^{137}Cs			
1	1165 (± 29)	45 (± 2)	51 (± 3)	25 (± 1)	4.51 (± 0.11)	3.62 (± 0.17)	12.56 (± 0.74)	$0.80*10^{-8}$ ($\pm 2.72*10^{-10}$)	Granitoids	Soft clay	795
2	948 (± 23)	36 (± 2)	51 (± 2)	13 (± 1)	3.67 (± 0.09)	2.93 (± 0.14)	12.56 (± 0.06)	$0.40*10^{-8}$ ($\pm 2.92*10^{-10}$)	Granitoids	Black soil	820
3	930 (± 42)	54 (± 3)	78 (± 5)	44 (± 2)	3.60 (± 0.16)	4.35 (± 0.21)	19.20 (± 0.15)	$1.38*10^{-8}$ ($\pm 5.52*10^{-10}$)	Gran./q.-diorites	Hard clay	657
4	1040 (± 24)	36 (± 2)	56 (± 3)	36 (± 1)	4.02 (± 0.09)	2.90 (± 0.14)	13.67 (± 0.63)	$1.12*10^{-8}$ ($\pm 3.67*10^{-10}$)	Granitoids	Soft clay	862
5	1260 (± 33)	44 (± 2)	76 (± 4)	31 (± 1)	4.87 (± 0.13)	3.54 (± 0.19)	18.82 (± 1.05)	$0.96*10^{-8}$ ($\pm 4.32*10^{-10}$)	Granitoids	Sandy	775
6	810 (± 22)	44 (± 2)	45 (± 3)	31 (± 1)	3.13 (± 0.08)	3.56 (± 0.16)	11.08 (± 0.69)	$0.96*10^{-8}$ ($\pm 3.94*10^{-10}$)	Granitoids	Black soil	1120
7	1220 (± 36)	43 (± 2)	68 (± 4)	17 (± 1)	4.72 (± 0.14)	3.47 (± 0.18)	16.63 (± 1.03)	$0.52*10^{-8}$ ($\pm 3.95*10^{-10}$)	Granitoids	Sandy	810
8	1160 (± 45)	52 (± 2)	64 (± 4)	32 (± 1)	4.49 (± 0.18)	4.22 (± 0.19)	15.67 (± 0.97)	$0.96*10^{-8}$ ($\pm 4.19*10^{-10}$)	Granitoids	Hard clay	680
9	1200 (± 41)	44 (± 2)	77 (± 3)	12 (± 1)	4.64 (± 0.16)	3.60 (± 0.20)	18.85 (± 0.75)	$0.37*10^{-8}$ ($\pm 3.55*10^{-10}$)	Granitoids	Sandy	821
10	1240 (± 51)	52 (± 3)	76 (± 5)	31 (± 2)	4.80 (± 0.20)	4.20 (± 0.23)	18.77 (± 1.18)	$0.96*10^{-8}$ ($\pm 5.76*10^{-10}$)	Gran./q.-diorites	Black soil	1003
11	1140 (± 57)	54 (± 3)	82 (± 5)	46 (± 1)	4.41 (± 0.22)	4.38 (± 0.26)	20.00 (± 1.28)	$1.43*10^{-8}$ ($\pm 3.71*10^{-10}$)	Gran./q.-diorites	Black soil	940
12	785 (± 38)	45 (± 2)	52 (± 3)	42 (± 1)	3.00 (± 0.14)	3.60 (± 0.17)	12.80 (± 0.76)	$1.32*10^{-8}$ ($\pm 4.49*10^{-10}$)	Quartz-diorites	Black soil	735
13	949 (± 26)	49 (± 1)	46 (± 3)	29 (± 1)	3.67 (± 0.10)	3.98 (± 0.12)	11.33 (± 0.68)	$0.89*10^{-8}$ ($\pm 2.76*10^{-10}$)	Porphyrites	Hard clay	722
14	865 (± 22)	47 (± 2)	60 (± 3)	23 (± 1)	3.35 (± 0.09)	3.84 (± 0.15)	14.82 (± 0.71)	$0.72*10^{-8}$ ($\pm 3.53*10^{-10}$)	Rose Granites	Black soil	1020
15	636 (± 18)	36 (± 2)	40 (± 3)	25 (± 1)	2.46 (± 0.07)	2.92 (± 0.14)	9.95 (± 0.63)	$0.78*10^{-8}$ ($\pm 3.82*10^{-10}$)	Gabbroids	Black soil	1123
16	643 (± 18)	33 (± 2)	39 (± 2)	22 (± 1)	2.49 (± 0.07)	2.68 (± 0.14)	9.66 (± 0.60)	$0.69*10^{-8}$ ($\pm 3.12*10^{-10}$)	Gabbroids	Black soil	1050
17	849 (± 22)	41 (± 2)	47 (± 2)	22 (± 1)	3.28 (± 0.09)	3.29 (± 0.14)	11.58 (± 0.57)	$0.69*10^{-8}$ ($\pm 3.24*10^{-10}$)	Quartz-diorites	Soft clay	920
18	1152 (± 27)	37 (± 2)	34 (± 2)	25 (± 1)	4.46 (± 0.10)	3.03 (± 0.14)	8.42 (± 0.55)	$0.77*10^{-8}$ ($\pm 3.70*10^{-10}$)	Marlstones	Soft clay	975
19	888 (± 23)	49 (± 2)	55 (± 3)	18 (± 1)	3.44 (± 0.09)	3.97 (± 0.17)	13.52 (± 0.69)	$0.57*10^{-8}$ ($\pm 2.11*10^{-10}$)	Marlstones	Soft clay	958
Range	636–1260	33–54	34–82	12–46	2.46–4.87	2.68–4.38	8.42–20.00	$0.37*10^{-8}$–$1.43*10^{-8}$			657–1123
Average	**994 (± 31)**	**44 (± 2)**	**58 (± 3)**	**27 (± 1)**	**3.84 (± 0.12)**	**3.58 (± 0.17)**	**14.20 (± 0.80)**	**$8.57*10^{-9}$ ($\pm 3.75*10^{-10}$)**			**883**
World median (UNSCEAR 2000)	**400**	**35**	**30**		**1.54**	**2.83**	**7.39**				

Outdoor absorbed dose rate in air (*D*)

As is known, the contribution of the natural radionuclide to the absorbed dose rate in air depends on the concentration of the radionuclide in the soil. Consequently, based on the determined results of activity concentrations of radionuclides in soil, the absorbed dose rate in air can be calculated. For this, Eq. (3) is used (UNSCEAR 2000):

$$D\ (nGy/h) = 0.0417A_K + 0.462A_U + 0.604A_{Th} \quad (3)$$

where D is the dose rate in the air at 1-m high from the ground; A_K, A_U, and A_{Th} are activity concentrations of ^{40}K, ^{238}U, and ^{232}Th respectively, determined from Eq. (1); and 0.0417, 0.462, and 0.604 are dose conversion factors for ^{40}K, ^{238}U, and ^{232}Th respectively;

From Table 3, presenting the calculation results for all radiological parameters, it is seen that results of outdoor absorbed dose rate vary from 66 to 122 nGy/h, with an average of 97 nGy/h. This average value is relatively higher than corresponding mean worldwide value of 57 nGy/h (UNSCEAR 2000). From Fig. 2, graphically presenting the components of absorbed dose rate, it is seen that ^{40}K makes the significant contribution to the formation of the outdoor absorbed dose rate in air.

Annual effective dose rate (*AEDR*)

To estimate the annual effective doses, it is necessary to take into account the conversion coefficient of 0.7 Sv/Gy from the absorbed dose in air to the effective dose received by adults, as well as the occupancy factors, which are 0.2 for outdoor and 0.8 indoor spaces respectively (UNSCEAR 2000). The effective dose rate is determined by using Eq. (4) (UNSCEAR 2000):

$$AEDR\ (mSv/y) = D \times Q \times T \times OF \times 10^{-6} \quad (4)$$

where D denotes the absorbed dose rate in the air, Q is the conversion coefficient, T is the time for 1 year, i.e., 8760 h, and OF is an occupancy factor.

From Table 3, it is observed that values of outdoor annual effective dose rate are in range from 0.08 to 0.15 mSv/y, with mean value of 0.12 mSv/y, which is higher than world global value of 0.07 mSv/y for outdoor annual effective dose rate (UNSCEAR 2000).

Radium equivalent activity (Ra_{eq})

Radium equivalent activity is determined taking into account the risks associated with the use of building materials that contain ^{40}K, ^{238}U, and ^{232}Th in acceptable quantities. Assuming that 130 Bq/kg of ^{40}K, 10 Bq/kg of ^{238}U, and 7 Bq/kg of ^{232}Th initiate almost the same dose of gamma radiation (Hussain and Hussain 2011), the sum of activity concentrations of ^{40}K, ^{238}U, and ^{232}Th is to be calculated. Radium equivalent activity is defined by the following formula (5) (Dhawal et al. 2013):

$$Ra_{eq}\ (Bq/kg) = 0.077A_K + A_U + 1.43A_{Th} \quad (5)$$

where A_K, A_U, and A_{Th} are activity concentrations of ^{40}K, ^{238}U, and ^{232}Th respectively. To reduce risks of irradiation, the material that has a radium equivalent activity greater than 370 Bq/kg, equivalent to a gamma dose of 1.5 mSv/y (UNSCEAR 2000), should not be used (Alaamer 2008; Dhawal et al. 2013). From Table 3, it is seen that calculated values for radium equivalent activity vary in range of 139–258 Bq/kg, with a mean value of 203 Bq/kg. All obtained values of radium equivalent activity are less than the limit value of 370 Bq/kg (UNSCEAR 2000).

Table 2 Comparison of the results obtained for ^{137}Cs with some data from other regions of the globe

#	Region/country	Activity concentrations of ^{137}Cs (Bq/kg)	References
1	Khrami Massif (Georgia)	4–33	(Kapanadze et al. 2019)
2	Mtskheta-Mtianeti region (Georgia)	0–53	(Kekelidze et al. 2017)
3	Kvemo Kartli region (Georgia)	0–88	(Kekelidze et al. 2018)
4	Rize Province (Turkey)	1–154	(Durusoy and Yildirim 2017)
5	Peshawar and Nowshera (Pakistan)	5–44	(Ismail et al. 2017)
6	Mirpur, Azad Kashmir (Pakistan)	1–3	(Rafique 2014)
7	İkizdere Valley (Turkey)	4–6	(Keser et al. 2013)
8	Kaptanpasa Valley (Turkey)	4–7	(Keser et al. 2013)
9	Vojvodina (Serbia)	6–55	(Forkapic et al. 2017)
10	Al-Baha (Saudi Arabia)	0–15	(Al-Zahrany and Al-Mogabes 2011)
11	Dzirula Massif (Georgia)	12–46	Present study

Table 3 Determined radiological parameters

Site #	D (nGy/h)	$AEDR$ (mSv/y)	Ra_{eq} (Bq/kg)	H_{ex}	H_{in}
1	100 (± 4)	0.12 (± 0.005)	207 (± 9)	0.56 (± 0.02)	0.68 (± 0.03)
2	87 (± 3)	0.11 (± 0.004)	182 (± 7)	0.49 (± 0.02)	0.59 (± 0.02)
3	111 (± 6)	0.14 (± 0.007)	237 (± 12)	0.64 (± 0.03)	0.79 (± 0.04)
4	93 (± 4)	0.11 (± 0.004)	195 (± 8)	0.53 (± 0.02)	0.62 (± 0.02)
5	119 (± 5)	0.15 (± 0.007)	250 (± 11)	0.68 (± 0.03)	0.79 (± 0.04)
6	81 (± 4)	0.10 (± 0.004)	171 (± 8)	0.46 (± 0.02)	0.58 (± 0.03)
7	111 (± 5)	0.14 (± 0.007)	233 (± 11)	0.63 (± 0.03)	0.75 (± 0.04)
8	111 (± 5)	0.14 (± 0.007)	232 (± 11)	0.63 (± 0.03)	0.77 (± 0.04)
9	117 (± 5)	0.14 (± 0.006)	246 (± 11)	0.66 (± 0.03)	0.79 (± 0.03)
10	122 (± 6)	0.15 (± 0.008)	256 (± 14)	0.69 (± 0.04)	0.83 (± 0.04)
11	122 (± 7)	0.15 (± 0.009)	258 (± 15)	0.70 (± 0.04)	0.84 (± 0.05)
12	85 (± 4)	0.10 (± 0.005)	180 (± 9)	0.48 (± 0.02)	0.61 (± 0.03)
13	90 (± 4)	0.11 (± 0.004)	188 (± 7)	0.51 (± 0.02)	0.64 (± 0.02)
14	94 (± 4)	0.12 (± 0.005)	200 (± 8)	0.54 (± 0.02)	0.67 (± 0.03)
15	68 (± 3)	0.08 (± 0.004)	143 (± 7)	0.39 (± 0.02)	0.48 (± 0.02)
16	66 (± 3)	0.08 (± 0.004)	139 (± 7)	0.37 (± 0.02)	0.46 (± 0.02)
17	83 (± 3)	0.10 (± 0.004)	173 (± 7)	0.47 (± 0.02)	0.58 (± 0.02)
18	86 (± 4)	0.11 (± 0.005)	175 (± 8)	0.47 (± 0.02)	0.57 (± 0.03)
19	93 (± 4)	0.11 (± 0.004)	196 (± 8)	0.53 (± 0.02)	0.66 (± 0.03)
Range	66–122	0.08–0.15	139–258	0.37–0.70	0.46–0.84
Average	**97 (± 4)**	**0.12 (± 0.005)**	**203 (± 9)**	**0.55 (± 0.02)**	**0.67 (± 0.02)**
World averages and limits (UNSCEAR 2000)	**57**	**0.07**	**< 370**	**< 1**	**< 1**

External and internal hazard indexes (H_{ex} and H_{in})

To assess the external effects of gamma radiation, a hazard index is commonly used, which is known as the external hazard index and is defined as follows (6.1) (Hussain and Hussain 2011):

$$H_{ex} = \frac{A_K}{4810} + \frac{A_U}{370} + \frac{A_{Th}}{259} \tag{6.1}$$

Another parameter, used in such calculations, is known as the internal hazard index, which is determined by the following way (6.2) (Hussain and Hussain 2011):

$$H_{in} = \frac{A_K}{4810} + \frac{A_U}{185} + \frac{A_{Th}}{259} \tag{6.2}$$

In Eqs. 6.1 and 6.2, A_K, A_U, and A_{Th} denote activity concentrations. According to limitations, hazard indexes should be less than one, which equals to radium equivalent activity of 370 Bq/kg (Kessaratikoon and Awaekechi 2008). In our case (Table 3), the average values of hazard indexes are 0.55 and 0.67 for H_{ex} and H_{in} respectively, which are less than the limit value.

Cancer risk

To calculate and estimate the fatal cancer risk (outdoor) to an individual living on the territory, the following Eq. (7) was used (Ramli et al. 2009):

$$\widehat{R}_i = aE_{out} \tag{7}$$

where a is the risk factor that is 0.05 of mortality per sievert, and E_{out} is outdoor effective annual dose rate. In our case, value of fatal cancer risk due to external gamma radiation is about 6.0×10^{-7} per year to each individual living in this region. This value is small and cannot serve the grounds for any concern.

Table 4 compares the results (average values) obtained for ^{40}K, ^{238}U, and ^{232}Th activity concentrations and air absorbed dose rate with similar results from different parts of the world.

Relationships

Based on the existing geological data and using ArcGIS tools, a geological map of the study area is created (Fig. 1). Using Kriging interpolation method, a spatial distribution scheme of the values of outdoor air absorbed dose rates is developed (Fig. 3).

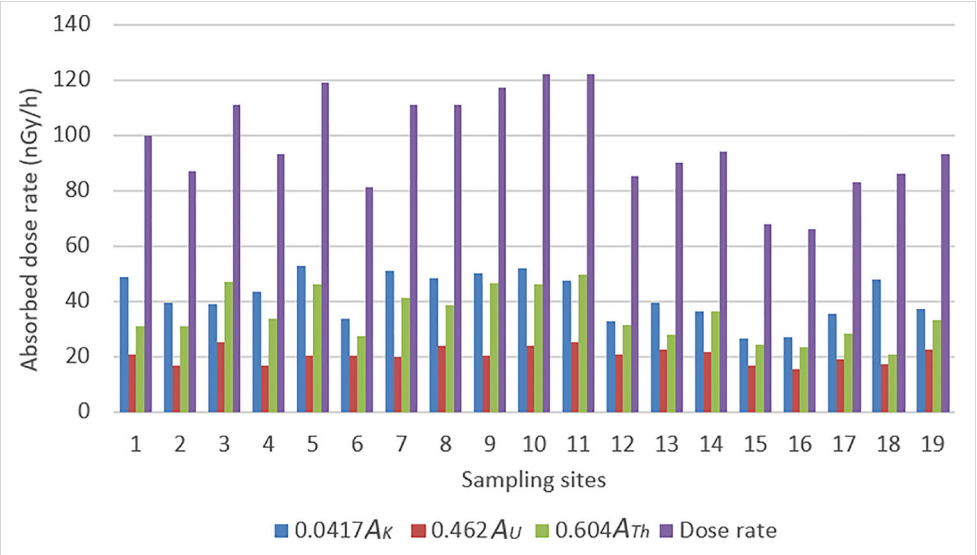

Fig. 2 Contribution of ^{40}K, ^{238}U, and ^{232}Th towards the dose rate

The analysis of Figs. 1 and 3 shows that the results of absorbed dose rates in the air (which in its turn is directly related to the concentrations of natural radionuclides in the soil) depend on the geology and topography of the territory. In particular, soils formed as a result of weathering of the Late Variscan granitoids of the Dzirula crystalline massif obviously reveal a higher level of natural radioactivity in contrast to the soils originated from sedimentary rocks. Gabbroids, as igneous mafic rocks, show a relatively low level of radioactivity. Consequently, it is apparent that the spatial distribution of natural radionuclides in the study area noticeably depends on the type of soil parent material.

Figure 4 demonstrates the relationship between the annual effective dose rate and petrology of the area (parent rocks) in accordance with sampling sites. According to the results, relatively increased values of annual effective dose can be observed. For instance, increased values are observed at the sites 3, 5, 10, and 11, which are associated with granite rocks. Relatively decreased values of annual effective dose rate are recorded for the sites 15, 16, 18, and 19 presenting gabbroidal and sedimentary rocks.

Conclusion

An analysis of the results shows that soils originated from sialic igneous rocks (granitoids in our case) revealed relatively high level of natural radioactivity than soils originated from mafic (gabbroids) or sedimentary rocks (marlstones). Results obtained for radionuclide concentrations, outdoor absorbed dose, and annual effective dose rate are slightly higher than the corresponding global averages. Consequently, terrestrial

Table 4 Comparison of average values of ^{40}K, ^{238}U, and ^{232}Th activity concentrations and absorbed dose rate with similar data from other regions of the world

#	Region/country	Activity concentrations (Bq/kg)			D (nGy/h)	References
		^{40}K	^{238}U	^{232}Th		
1	Chakwal (Pakistan)	558	31	48	66	(Mehdi et al. 2016)
2	South Konkan (India)	196	45	59	67	(Dhawal et al. 2013)
3	Rize Province (Turkey)	345	25	52	57	(Durusoy and Yildirim 2017)
4	Kaptanpasa Valley (Turkey)	607	19	24	51	(Keser et al. 2013)
5	Najaf Governorate (Iraq)	277	268	7	140	(Hussain and Hussain 2011)
6	Riyadh city (Saudi Arabia)	225	15	11	23	(Alaamer 2008)
7	Songkhla (Thailand)	213	68	45	68	(Kessaratikoon and Awaekechi 2008)
8	Nile Delta (Egypt)	45	9	6	10	(Yousef et al. 2007)
9	Sitakunda (Bangladesh)	468	31	62	71	(Rahman et al. 2012)
10	Al-Baha (Saudi Arabia)	298	10	9	22	(Al-Zahrany and Al-Mogabes 2011)
11	Dzirula Massif (Georgia)	994	44	58	97	Present study

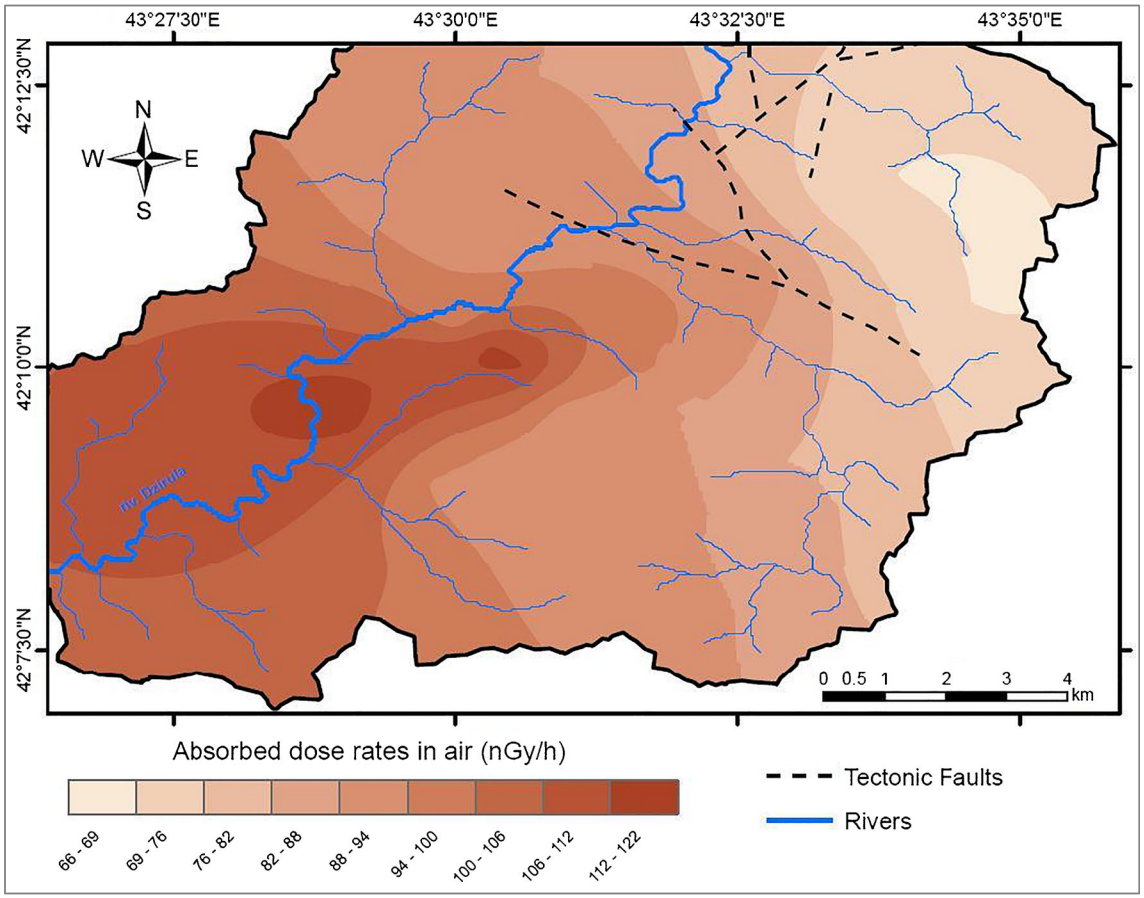

Fig. 3 Spatial distribution of the outdoor absorbed dose rates in air

gamma radiation of the study area, of course, is not life threatening, but deserves certain attention and maybe further investigation.

According to results obtained, average value of radium equivalent activity equals to 203 Bq/kg, which is less than internationally established limit of 370 Bq/kg (UNSCEAR 2000). Considering that in the area under study there is no deep regional tectonic fault, it can be concluded that territory is free from the hazards due to radium and its progeny radon. All values obtained for external and internal hazard indexes

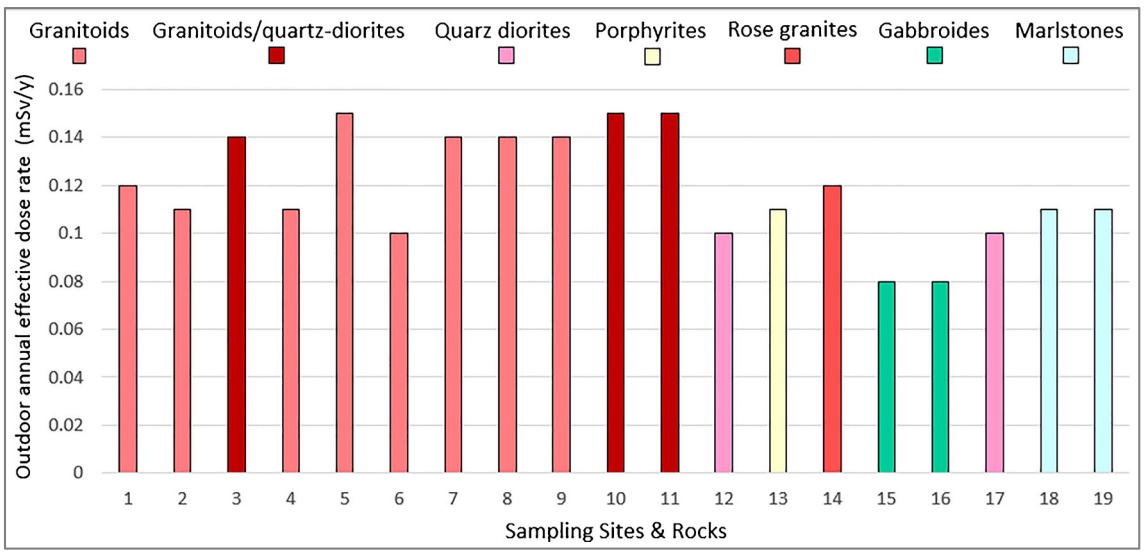

Fig. 4 Relationship between annual effective dose and petrology of the area

are less than unity. This indicates that the population living in the study area is not exposed to radiation exceeding permissible limits.

Results of natural radionuclide concentrations provided in Table 1 do not significantly differ from the results previously obtained for the Khrami crystalline massif, where average values of activity concentrations are 880, 39, and 53 Bq/kg for ^{40}K, ^{238}U, and ^{232}Th respectively (Kapanadze et al. 2019). This apparently shows some similarities between these two crystalline missifs in terms of natural radioactivity.

The results of the study can serve to develop unified analytical information base on the levels of natural radioactivity and radiation pollution of the environment and can be used during the planning of different social-economic projects.

Funding This work has been supported by the Shota Rustaveli National Science Foundation (SRNSF) (grant number: PHDF-19-298; project title: Study of distribution of natural radionuclides in soils and assessment of radiation hazards on the example of Imereti region (Georgia)).

Declarations

Conflict of interest The authors declare that they have no competing interests.

References

Adamia S, Zakariadze G, Chkhotua T, Sadradze N, Tsereteli N, Chabukiani A, Gventsadze A (2011) Geology of the Caucasus: a review. Turk J Earth Sci 20:489–544

Alaamer AS (2008) Assessment of human exposures to natural sources of radiation in soil of Riyadh, Saudi Arabia. Turk J Eng Environ Sci 32(4):229–234

Al-Zahrany AA, Al-Mogabes KS (2011) Measurement of concentrations of the natural radio-activities and Cs-137 in soil samples in the Al-Baha region of Saudi Arabia. WIT Trans Ecol Environ 144. https://doi.org/10.2495/ECO110381

Dhawal SJ, Kultarni GS, Pawar SH (2013) Terrestrial background radiation studies in South Konkan, Maharashtra, India. Int J Radiat Res 11(4):263–270

Durusoy A, Yildirim M (2017) Determination of radioactivity concentrations in soil samples and dose assessment for Rize Province, Turkey. J Radiat Res Appl Sci 10:348–352

Forkapic S, Vasin J, Bikit I, Mrdja D, Bikit K, Milić S (2017) Correlatons between soil characteristics and radioactivity content of Vojvodina soil. J Environ Radioact 166(Pt1):104–111. https://doi.org/10.1016/j.jenvrad.2016.04.003

Geguchadze S, Davlianidze G, Sekhnianidze G, Shiriashvili O, Khabelashvili A, Iagjian R (1972) Geological map (K-38-64-A). State geological founds of Georgia

Hussain RO, Hussain HH (2011) Natural occurring radionuclide materials. In: Singh N (ed) Radioisotopes - Applications in Physical Sciences. InTech. https://doi.org/10.5772/20562

Ismail M, Zia MA, Khan HM (2017) Investigation of Cs-137 in the environmental soil segments of the Peshawar and Nowshera districts of Khyber Pakhtunkhwa, Pakistan. Int J Radiat Res 15(4):407–412

Kapanadze K, Magalashvili A, Imnadze P (2019) Distribution of natural radionuclides in the soils and assessment of radiation hazards in the Khrami Late Variscan crystal massif (Georgia). Heliyon 5(3): e01377. https://doi.org/10.1016/j.heliyon.2019.e01377

Kekelidze N, Jakhutashvili T, Tutberidze B, Tulashvili E, Akhalkatsishvili M, Mtsariashvili L (2017) Radioactivity of soils in Mtskheta-Mtianeti region (Georgia). Ann Agrar Sci 15(3):304–311

Kekelidze N, Jakhutashvili T, Tutberidze B, Tulashvili E, Akhalkatsishvili M, Mtsariashvili L (2018) Radionuclides in samples of soil of different types in the Kvemo Kartli region (Georgia). Int J Agricult Biosyst Eng 3(3):57–67

Keser R, Korkmaz Görür F, Alp İ, Okumusoğlu NT (2013) Determination of radioactivity levels and hazards of sediment and rock samples in İkizdere and Kaptanpasa Valley, Turkey. Int J Radiat Res 11(3):155–165

Kessaratikoon P, Awaekechi S (2008) Natural radioactivity measurement in soil samples collected from municipal area of Hat Yai district in Songkhla province, Thailand. KMITL Sci J 8(2):52–58

Knoll GF (1989) Radiation detection and measurement, Second edn. John Wiley & Sons, Inc, New York

Mehdi SA, Rahman SU, Khan K, Jabbar A, Rafique M (2016) Assessment of annual effective dose from measured soil radioactivity levels using HPGe detector. Univ J Eng Sci 4(4):79–83. http://www.hrpub.org. https://doi.org/10.13189/ujes.2016.040403

Rafique M (2014) Cesium-137 actvity concentratons in soil and brick samples of Mirpur, Azad Kashmir; Pakistan. Int J Radiat Res 12(1):39–46

Rahman MM, Islam AT, Kamal M, Chowdhury MI (2012) Radiation hazards due to terrestrial radionuclides at the coastal area of Ship Breaking Industries, Sitakunda, Bangladesh. Sci J Phys. ISSN: 2276-6367. https://doi.org/10.7237/sjp/211

Ramli AT, Apriantoro NH, Wagiran H (2009) Assessment of radiation dose rates in the high terrestrial gamma radiation area of Selama District, Perak, Malaysia. Appl Phys Res 1(2). https://doi.org/10.5539/apr.v1n2p45

UNSCEAR (2000) United Nations Scientific Committee on the Effects of Atomic Radiation. Annex B. Exposures from Natural Radiation Sources, New York

Urushadze T, Tkhelidze A, Gambashidze G, Tsereteli G, Kubaneishvili N (2015) Soils of Georgia. UNDP Georgia

Yousef ML, Abu El-Ela A, Eousef HA (2007) Natural radioactivity levels in surface soil of Kitchener Drain in the Nile Delta of Egypt. J Nucl Radiat Phys 2(1):61–68